

Two fossil groups of galaxies at $z \approx 0.4$ in the COSMOS: accelerated stellar-mass build-up, different progenitors

D. Pierini^{1*}, S. Giodini², A. Finoguenov¹, H. Böhringer¹, E. D’Onghia³,
G. W. Pratt⁴, J. Démoclès⁴, M. Pannella⁴, S. Zibetti⁵, F. G. Braglia⁶,
M. Verdugo¹, F. Ziparo¹, A. M. Koekemoer⁷, M. Salvato^{8,9,1}
and the COSMOS Collaboration

¹Max-Planck-Institut für extraterrestrische Physik, Giessenbachstrasse, D-85748, Garching bei München, Germany

²Leiden Observatory, P.O. Box 9513, NL-2300 RA Leiden, The Netherlands

³Harvard-Smithsonian Center for Astrophysics, 60 Garden Street, Cambridge, MA 02138, U.S.A.

⁴Laboratoire AIM, DAPNIA/Service d’Astrophysique, CEA/DSM, CNRS, Université Paris Diderot, Bât. 709, CEA-Saclay, F-91191 Gif-sur-Yvette Cedex, France

⁵Dark Cosmology Centre, Niels Bohr Institute, University of Copenhagen, Juliane Maries Vej 30, 2100 Copenhagen Ø, Denmark

⁶Department of Physics and Astronomy, University of British Columbia, 6224 Agricultural Road, V6T 1Z1 Vancouver BC, Canada

⁷Space Telescope Science Institute, 3700 San Martin Drive, Baltimore MD 21218, U.S.A.

⁸Max-Planck-Institut für Plasmaphysik, Boltzmannstrasse 2, D-85748 Garching, Germany

⁹Caltech, 1200 East California Blvd, PMA 249-17, Pasadena, CA 91125, USA

Accepted ... Received ...; in original form ...

ABSTRACT

We report on two fossil groups of galaxies at redshifts $z = 0.425$ and 0.372 discovered in the Cosmic Evolution Survey (*COSMOS*) area. Selected as X-ray extended sources, they have total masses (M_{200}) equal to $1.9 (\pm 0.41) \times 10^{13}$ and $9.5 (\pm 0.42) \times 10^{13} M_{\odot}$, respectively, as obtained from a recent X-ray luminosity–mass scaling relation. The lower mass system appears isolated, whereas the other sits in a well-known large-scale structure (LSS) populated by 27 other X-ray emitting groups. The identification as fossil is based on the i -band photometry of all the galaxies with a photometric redshift consistent with that of the group at the 2σ confidence level and within a projected group-centric distance equal to $0.5R_{200}$, and $i_{AB} \leq 22.5$ mag limited spectroscopy. Both fossil groups exhibit high stellar-to-total mass ratios compared to all the X-ray selected groups of similar mass at $0.3 \leq z \leq 0.5$ in the *COSMOS*. At variance with the composite galaxy stellar mass functions (GSMFs) of similarly massive systems, both fossil group GSMFs are dominated by passively evolving galaxies down to $M^{stars} \sim 10^{10} M_{\odot}$ (according to the galaxy broad-band spectral energy distributions). The relative lack of star-forming galaxies with $10^{10} \leq M^{stars} \leq 10^{11} M_{\odot}$ is confirmed by the galaxy distribution in the $b - r$ vs i colour–magnitude diagram. Hence, the two fossil groups appear as more mature than the coeval, similarly massive groups. Their overall star formation activity ended rapidly after an accelerated build up of the total stellar mass; no significant infall of galaxies with $M^{stars} \geq 10^{10} M_{\odot}$ took place in the last 3 to 6 Gyr. This similarity holds although the two fossil groups are embedded in two very different density environments of the LSS, which suggests that their galaxy populations were shaped by processes that do not depend on the LSS. However, their progenitors may do so. We discuss why the late merging of a compact group is favoured over the early assembly as a formation scenario for the isolated, low-mass fossil group.

Key words: X-rays: galaxies: clusters – galaxies: groups: general – galaxies: evolution – galaxies: luminosity function, mass function.

1 INTRODUCTION

In early numerical simulations, the merging of a compact galaxy group was found to lead to the formation of a single

* Currently guest astronomer at the MPE

elliptical galaxy (hence a “fossil group”) in a few billion years (Barnes 1989)¹. The final product retains an X-ray emitting halo of hot gas (Ponman & Bertram 1993). The whole scenario was proved to be plausible by the discovery of the fossil group RX J1340.6+4018 (Ponman et al. 1994).

The standard observational definition of a fossil system is based on the existence of extended X-ray emission with a bolometric luminosity $L_X > 10^{42} h_{50}^{-2} \text{ erg s}^{-1}$ and of an R-band magnitude gap $\Delta m_{12} > 2$ between the brightest and second brightest members within $0.5R_{200}$ ² (Jones, Ponman & Forbes 2000). In theoretical studies, the analogous definition of a fossil system is less straightforward (see e.g., D’Onghia et al. 2005 for a discussion).

On the basis of the existing observations, mostly limited to the local Universe, fossil groups are expected to be a considerable population among the gravitationally bound systems of galaxies (Vikhlinin et al. 1999; Romer et al. 2000; Jones et al. 2003; La Barbera et al. 2009; Voevodkin et al. 2010). For instance, their estimated spatial density is equal to $2.83 \times 10^{-6} h_{75}^3 \text{ Mpc}^{-3}$ for an X-ray bolometric luminosity above $0.89 \times 10^{42} h_{75}^{-2} \text{ erg s}^{-1}$ (La Barbera et al. 2009). X-ray properties and dark-matter (DM) content of fossil groups are comparable to those of bright groups and poor clusters of galaxies, with total masses of $\sim 10^{13} - 10^{14} M_\odot$, whereas their brightest members are typically as luminous as a cluster cD galaxy ($M_R < -22.5 + 5 \log h_{50}$).

In recent high-resolution hydrodynamical cosmological simulations in a Λ cold dark matter (Λ CDM) universe, fossil groups have already assembled half of their final mass at redshifts $z \geq 1$, and subsequently they typically grow by minor mergers only, whereas non-fossil systems of similar total mass on average form later (D’Onghia et al. 2005; Dariush et al. 2007). The early assembly leaves sufficient time for galaxies with a luminosity $L \geq L^*$ (assuming a Schechter 1976 luminosity function) to merge into the central galaxy by dynamical friction, which yields the magnitude gap defining fossil groups. This “early formation” scenario is alternative to the compact group merging scenario (Barnes 1989).

However, no difference seems to exist in the distribution of neighboring faint galaxy density excess, distance from the red sequence³, structural parameters, or stellar population properties between the brightest central galaxies (BCGs) in 25 fossil groups at $z \leq 0.1$ and a sample of bright field ellipticals with a similar distribution in optical luminosity and X-ray properties (La Barbera et al. 2009). These authors argue that this evidence undermines the idea that fossil systems represent the “end product” of a physical mechanism

that occurred at high redshift; it rather suggests that fossil groups are the final stage of mass assembly in the Universe.

Whether either interpretation is true or fossil groups correspond to a transient phase in the life of a galaxy group (von Benda-Beckmann et al. 2008; Dariush et al. 2010; Cui et al. 2011), whether they form a distinct family of groups (D’Onghia & Lake 2004; Khosroshahi, Ponman & Jones 2007) or not (Sales et al. 2007; Zibetti, Pierini & Pratt 2009; Sun et al. 2009; Démoclès et al. 2010; Voevodkin et al. 2010; Cui et al. 2011), for several reasons it is important to extend the present knowledge of fossil systems beyond the local Universe and towards lower total masses.

If undisturbed for a very long time, fossil groups may represent the ultimate example of hydrostatic equilibrium in virialized systems (Vikhlinin et al. 1999). This conclusion is supported by a recent detailed study of two such systems based on high-quality XMM-Newton spectro-imaging data (Démoclès et al. 2010).

In addition, fossil groups could represent the least massive, baryonically closed systems (Mathews et al. 2005), their baryon mass fraction being equal to the cosmic mean value⁴. If so, they could form a reference sample with a recent, quiescent merging activity with which one can investigate the origin of the average baryon deficiency within R_{500} ($\approx 0.7R_{200}$) found in X-ray emitting groups at $z \leq 1$ (Giodini et al. 2009, hereafter referred to as G09; see also Teyssier et al. 2011). In particular, two pair-matched samples of fossil groups with a range in total mass and redshift, one with radio-loud BCGs and the other with radio-quiet BCGs, could be used to estimate the “instantaneous” boost of the entropy in the central regions of the ICM that is due to radio-galaxy feedback (cf. Giodini et al. 2010).

From simple considerations on the hierarchical nature of structure growth via merging (Milosavljević et al. 2006), fossil systems are expected to be more frequent (by a factor of ten) at the group mass-scale than at the cluster mass-scale ($\sim 10^{14} - 10^{15} M_\odot$). This is confirmed by the most recent study of fossil groups based on hydrodynamical resimulations of five regions in the Millennium Simulation and on galaxy formation models (Cui et al. 2011 and references therein). Therefore fossil groups may also help in understanding the properties of more massive bound systems at $z = 0$, especially if it turns out that they foster the formation of the most massive progenitor of the BCG of a cluster, as suggested by J 0454–0309 at $z = 0.26$ (Schirmer et al. 2010; cf. Barnes 1989 and references therein).

During our ongoing studies of the X-ray selected groups in the 2 deg^2 area of the Cosmic Evolution Survey (*COSMOS*; Scoville et al. 2007), we have discovered two fossil groups at $z = 0.372$ and $z = 0.425$. As demonstrated by G09 and Giodini et al. (2010), the multi-wavelength data set of the *COSMOS* offers a thus far unique opportunity to characterize X-ray selected groups of galaxies up to $z \sim 1$. This enables us not only to fully describe the galaxy populations of the two fossil groups, but also to characterize their

¹ These numerical simulations adopted a 1:4 ratio of luminous to dark matter and assumed that individual galaxies had dark halos.

² R_Δ is the radius within which the total mass density of a group/cluster is equal to Δ times the critical density of the Universe (ρ_c). Correspondingly, $M_\Delta = \Delta \rho_c(z) (4\pi/3) R_\Delta^3$ is the total mass enclosed by R_Δ .

³ In a given colour-magnitude diagram, the red sequence is the locus populated by galaxies dominated by old, passively evolving, stellar populations (see Arimoto & Yoshii 1987). This locus is particularly tight if the two broad-band filters that define the colour bracket the so-called 4000 Å break. Among coeval galaxies, the old, passively evolving ones exhibit the reddest colours, if dust attenuation is neglected (see Pierini et al. 2004 for a discussion).

⁴ The cosmic mean value of the baryon mass fraction can be obtained e.g. from the five years measurements of the Cosmic Microwave Background (CMB) performed with the *Wilkinson Microwave Anisotropy Probe* (*WMAP5*; Dunkley et al. 2009). According to this estimate, it amounts to 0.171 ± 0.009 .

surrounding large-scale structures (LSSs), and to speculate on their progenitors. In Sect. 2 we describe selection and properties of these two groups. Their galaxy stellar mass functions and colour–magnitude diagrams are determined in Sect. 3. Discussion of results and inference on evolutionary scenarios appear in Sect. 4; conclusions are drawn in Sect. 5.

As in G09, we adopt a Λ CDM cosmological model ($\Omega_m = 0.258$, $\Omega_\Lambda = 0.742$) with $H_0 = 72 \text{ km s}^{-1} \text{ Mpc}^{-1}$, consistently with results from *WMAP5* (Dunkley et al. 2009; Komatsu et al. 2009). Thus, a redshift of 0.372 (0.425) corresponds to a lookback time of 3.981 Gyr (4.409 Gyr), a luminosity distance of 1961.1 Mpc (2298.2 Mpc), an angular diameter distance of 1041.8 Mpc (1131.8 Mpc), and a scale of 5.051 kpc'' (5.487 kpc'').

Hereafter magnitudes are expressed in the AB system unless otherwise noted.

2 SAMPLE SELECTION AND PROPERTIES

From the composite mosaic of the *XMM-Newton* and *Chandra* X-ray data mapping the *COSMOS* 2 deg² area, extended sources (i.e., groups and clusters) were detected down to a flux limit of $10^{-15} \text{ erg s}^{-1} \text{ cm}^{-2}$ (Finoguenov et al. in preparation; see also Finoguenov et al. 2007). G09 selected 91 groups/poor clusters at $0.1 < z < 1$, which have an X-ray flux estimate at a significance better than 3σ , after point-like source subtraction (see Finoguenov et al. 2007). For these groups, the membership of a galaxy (through a precise photometric redshift⁵) and the total stellar mass in galaxies together with its uncertainty were robustly determined as described in G09. The total mass of each group was determined from the L_X – M_{200} relation established through weak lensing analysis by Leauthaud et al. (2010). Uncertainties on M_{200} are statistical only (i.e., they arise from the L_X – M_{200} relation). The effects of systematics are estimated to be lower than the statistical uncertainty⁶.

We searched for fossil groups in the G09 sample. As in Giodini et al. (in preparation), we defined as member candidates of a group those galaxies within a projected group-centric distance of R_{200} , and with a photometric redshift consistent with the photometric redshift of the group within two times the uncertainty on the photometric redshift of the group. Then we inspected the brightest member-candidate galaxies within a projected group-centric distance equal to $0.7R_{200}$ to minimize the potential bias produced by uncertainties on R_{200} . As for ranking in luminosity, the available i -band photometry was considered, since the reference

COSMOS photometric catalogue is extracted from imaging in this band (Ilbert et al. 2009). This choice avoids the use of template- and (photometric) redshift-dependent k -corrections as for the choice of considering rest-frame R-band magnitudes. Furthermore, up to $z = 1$, the i -filter (observed frame) maps emission at rest-frame wavelengths redder than the 4000 Å-break, which limits the impact of young stellar populations and, potentially, attenuation by a dusty interstellar medium.

A number of groups were initially selected as potential fossil systems, the magnitude difference between the BCG and any other bright member-candidate galaxy within $0.7R_{200}$ being conservatively chosen to be larger than 1.5 i -mag. We set a larger search radius and a smaller magnitude gap than those required by the definition of fossil groups (cf. Sect. 1) in order to maximize the number of candidates in this first round of the search for fossil groups. Two groups were successively established as fossil thanks to the existing spectroscopic information (Lilly et al. 2007), limited to sources brighter than $i = 22.5$ mag, which enabled a finer screening against projected foreground/background bright galaxies.

On one hand, we flagged out galaxies classified as member candidates if they were located within R_{200} from the X-ray centroid of either fossil group but exhibited a line-of-sight velocity in excess of 3000 km s^{-1} plus its 3σ uncertainty⁷ with respect to the spectroscopically determined recession velocity of either group. The redshift of each group was computed using the median spectroscopic redshifts of the galaxies within R_{200} through iterative removal of outliers with a recession velocity beyond 1500 km s^{-1} with respect to the recession velocity of the group. The starting redshift was defined by the photometric redshifts of galaxies on the red sequence. Contamination was checked by running a red-sequence-finding algorithm between redshifts 0 and 2 and by using spectroscopic group catalogs (Knobel et al. 2009). On the other hand, the available spectroscopy enabled us to check, in particular, that bright galaxies within $0.5R_{200}$ from the X-ray centroid of either fossil group were actually not dropped as member candidates because of an inaccurate photometric redshift. Additional considerations on size and luminosity were used to check the goodness of the photometric redshifts of relatively bright galaxies without spectroscopy (see CXGG 095951+0212.6 in Fig. 2).

Figures 1 and 2 show cut-outs of the central regions of the two *COSMOS* fossil groups under study, which encompass the area within $0.5R_{200}$ for each system. They reproduce X-ray surface brightness contours overlaid on the i -band HST/ACS images (Koekemoer et al. 2007) of the two galaxy systems. In particular, member candidates (i.e., photometric members) are indicated together with all galaxies brighter than $i = 22.5$ mag having a spectroscopic redshift. The BCG of either group can be easily identified at the center of the X-ray emission region.

One system, CXGG 095951+0140.8, has $\Delta m_{i12} = 2.19 \pm 0.014$ mag (i.e., $\Delta m_{12} = 2.10 \pm 0.02$ mag as obtained from the difference between the magnitudes in the rest-frame r -band), $R_{200} = 832 \pm 19.6$ kpc, $M_{200} = 9.5 (\pm 0.42) \times$

⁵ For galaxies with $i \leq 25$ mag at the redshift of the two fossil groups under study (i.e., $z \approx 0.4$), the 1σ error on the photometric redshift is equal to $0.03 \times (1 + z) = 0.042$.

⁶ Systematic effects tested were: errors on photometric redshifts, mis-centering, uncertainties in the mass–concentration relation. These amount to a few percents (see fig. 7 in Leauthaud et al. 2010), while the statistical error is much larger. Removal of point-like sources can lead to underestimate the X-ray flux, since the scale at which they are removed matches with the scale of cool-cores. The correction, as detailed in sect. 4.2 of Leauthaud et al. (2010), amounts to 3–17% of the total X-ray flux. This correction was taken into account when establishing the L_X – M_{200} relation.

⁷ The uncertainty of the high-quality (flags 3 and 4) zCOSMOS spectroscopic redshifts amounts to 110 km s^{-1} .

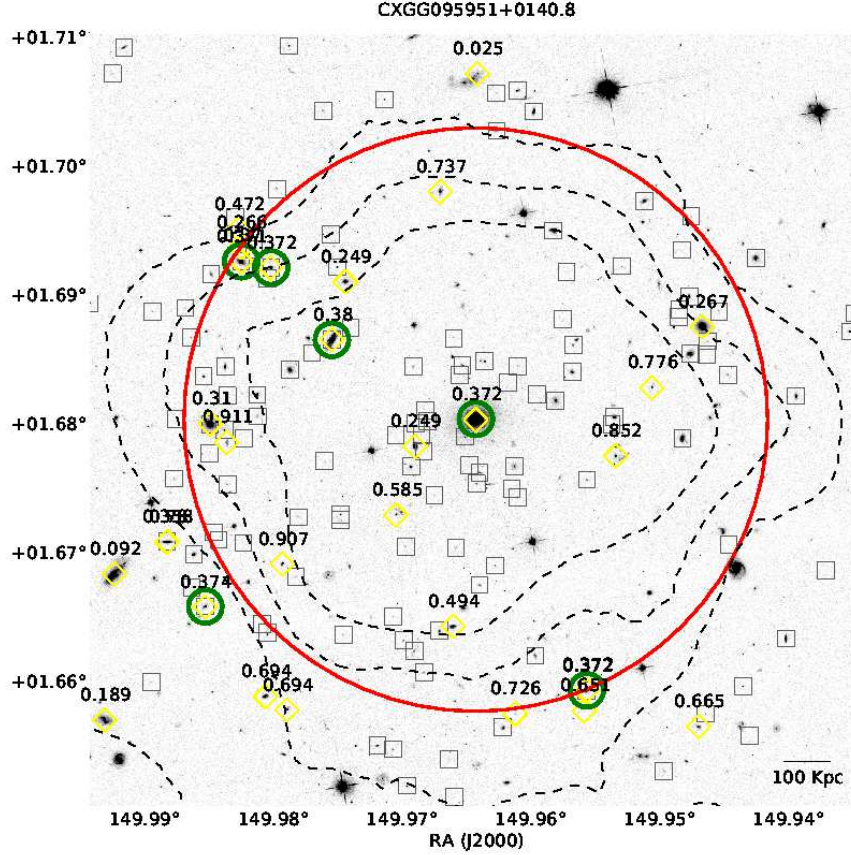


Figure 1. *i*-band image of CXGG 095951+0140.8, enclosing a circular area of radius $0.5R_{200}$ centered on the X-ray position of the group (marked in red). Photometric members are marked with squares; green circles mark the spectroscopic members. Available spectroscopic redshifts of all objects in the region are given (yellow diamonds). Dashed contours indicate values of the X-ray surface brightness at the 4σ , 7σ and 10σ levels after removal of point-like sources, where 1σ corresponds to $4.6 \times 10^{-16} \text{ erg s}^{-1} \text{ cm}^{-2} \text{ arcmin}^{-2}$ in the 0.5–2 keV band.

$10^{13} M_{\odot}$, $z = 0.372$, and six spectroscopic members. It is part of a large-scale structure (see fig. 1 in G09 and fig. 3 in Scoville et al. 2007) populated by 28 X-ray emitting groups distributed across the entire 2 deg^2 area of the *COSMOS* (corresponding to a cross size of about 25.5 Mpc at $z = 0.37$). Furthermore, its dominant galaxy (with a rest-frame absolute magnitude $M_i = -24.87$) hosts a point-like radio source (see Giodini et al. 2010). The other fossil group, CXGG 095951+0212.6, has $\Delta m_{12} = 2.35 \pm 0.014 \text{ mag}$ (i.e., $\Delta m_{12} = 2.32 \pm 0.02 \text{ mag}$ in the rest-frame *r*-band), $R_{200} = 478 \pm 54.4 \text{ kpc}$, $M_{200} = 1.9 (\pm 0.41) \times 10^{13} M_{\odot}$, $z = 0.425$, and eight spectroscopic members. It is isolated and its BCG has $M_i = -23.87$.

Basic properties of the two fossil groups under study are listed in Table 1. In addition, we note that they populate the upper half of the distribution of the *COSMOS* X-ray selected groups in the (galaxy) stellar mass fraction–group total-mass diagram (G09, their fig. 5), where quan-

tities are estimated at $0.7R_{200}$. This is particularly true for CXGG 095951+0212.6. As from G09⁸, the stellar mass fraction is equal to 0.039 for the more massive fossil group (CXGG 095951+0140.8) and 0.143 for the less massive one (CXGG 095951+0212.6). Thus, the fraction of the stellar

⁸ Giodini et al. (in preparation) use a new catalogue of galaxy stellar masses by O. Ilbert instead of the catalogue by Ilbert et al. (2009) used in G09. The difference between the catalogues rests on the way stellar masses are computed. In the new one, stellar mass estimates are based on fitting the spectral energy distribution (SED) of a galaxy and not on the rest-frame K-band luminosity of the latter; furthermore, the stellar initial mass function of Chabrier (2003) is used instead of a Salpeter (1955) one. For the purposes of our study it is important that no systematics differently affects such estimates in fossil and non-fossil groups, not that the absolute scale of the estimated stellar mass of a galaxy is correct.

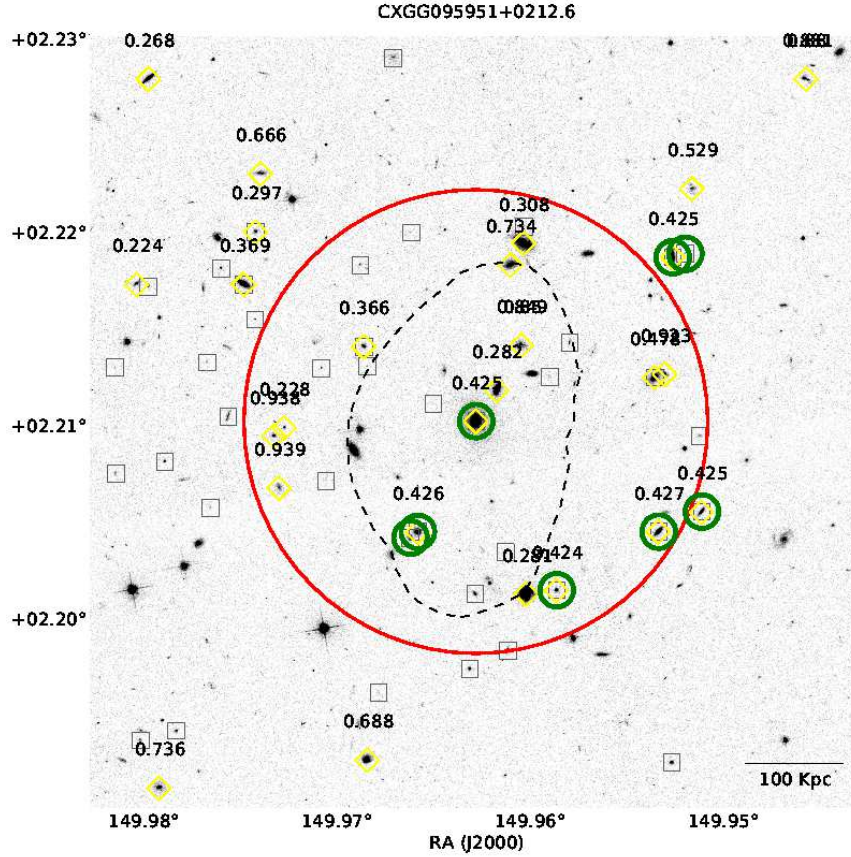


Figure 2. The same as in Fig. 1 but for CXGG 095951+0212.6. Here the 1σ value of the X-ray surface brightness corresponds to $3.5 \times 10^{-16} \text{ erg s}^{-1} \text{ cm}^{-2} \text{ arcmin}^{-2}$ in the 0.5–2 keV band.

mass in galaxies decreases with increasing total mass for the two fossil groups as for all other coeval groups (G09).

Furthermore, the more (less) massive fossil group exhibits a value of the total i -band-to-X-ray luminosity ratio at R_{200} (L_i/L_X) equal to 138 (305), after background subtraction including spectroscopic information (from Giodini et al. in preparation). Therefore CXGG 095951+0140.8 (CXGG 095951+0212.6) exhibits a low (normal) value for its total mass with respect to the distribution of L_i/L_X as a function of M_{200} for the 51 groups at $z = 0.3$ – 0.5 considered by Giodini et al.⁹.

With a total mass of $1.9 (\pm 0.41) \times 10^{13} M_\odot$, CXGG 095951+0212.6 is among the least massive fossil systems selected in X-rays, whereas CXGG 095951+0212.6 is at the boundary between the group and cluster mass regimes (cf. Vikhlinin et al. 1999; Sun et al. 2009; Zibetti et al. 2009; Démoclès et al. 2010; Voevodkin et al. 2010). As a reference, RX J105453.3+552102 at $z = 0.47$, with a total mass

of $\sim 10^{15} M_\odot$ (Aguerre et al. 2011), is among the most massive fossil systems¹⁰.

¹⁰ RX J105453.3+552102 is not considered as a fossil system by Aguerri et al. (2011), since its magnitude gap is equal to 1.92 ± 0.09 mag in the observed-frame r -band. The bright end of the galaxy luminosity function of this cluster is populated by old, passively evolving objects (Aguerre et al. 2011), so that the introduction of a k -correction is expected not to significantly modify the magnitude gap in the rest-frame r -band. However, the fossil criteria fixed by Jones et al. (2003) are somewhat arbitrary and depend on the way magnitudes are measured (see Aguerri et al. 2011 for a discussion). In addition, the likely contribution from diffuse light to the BCG emission is hard to be fully accounted for (see Zibetti et al. 2009 for a discussion). Thus, we consider RX J105453.3+552102 as a fossil system as we did for RXC J2315.7–0222 at $z = 0.026$ with $\Delta m_{12} = 1.88 \pm 0.03$ mag in the rest-frame R_C -band (Démoclès et al. 2010).

⁹ These COSMOS X-ray selected groups define a mass-complete sample, probing different large-scale density environments.

Table 1. Basic properties of the sample

Denomination	z	M_{200} [$10^{13} M_{\odot}$]	R_{200} [kpc]	Δm_{i12} [mag]	Δm_{12} [mag]	N	N_{phot}	N_{spec}
CXGG 095951+0140.8	0.372	9.5 ± 0.42	832 ± 19.6	2.19 ± 0.014	2.10 ± 0.02	261	140	6
CXGG 095951+0212.6	0.425	1.9 ± 0.41	478 ± 54.4	2.35 ± 0.014	2.32 ± 0.02	68	29	8

Denomination, spectroscopic redshift (z), total mass (M_{200}), size (R_{200}), observed i -band and rest-frame r -band magnitude gaps between the first two brightest member galaxies (Δm_{i12} and Δm_{12} , respectively), total number of galaxies brighter than the completeness magnitude ($i = 25.37$ mag and $i = 25.17$ mag for CXGG 095951+0140.8 and CXGG 095951+0212.6, respectively) within R_{200} (N), numbers of expected (i.e., the photometric members after statistical subtraction of field galaxies) and spectroscopic member galaxies within R_{200} (N_{phot} and N_{spec} , respectively) are listed for each fossil group.

3 RESULTS

3.1 Galaxy stellar mass function

We compute the galaxy stellar mass function (GSMF) of the two fossil groups in bins of 0.5 dex in stellar mass (M^{stars}). Only member-candidate galaxies with a stellar mass above the completeness mass at the redshift of each group are considered. The completeness mass is equal to $8.3 \times 10^8 M_{\odot}$ or $1.25 \times 10^9 M_{\odot}$ for, respectively, all member-candidate galaxies of CXGG 095951+0212.6 or those among them that are classified as passively evolving¹¹. It is equal to $3 \times 10^8 M_{\odot}$ or $5 \times 10^8 M_{\odot}$ for, respectively, all member-candidate galaxies of CXGG 095951+0140.8 or the passively evolving ones among them.

We applied a correction for the expected number of interlopers, based on the statistics of the galaxies outside X-ray emitting bound structures in the same photometric-redshift slice, which define the coeval field of either group. This holds whether or not galaxies are additionally selected according to their star formation activity. In each case, the field GSMF was normalized by the group-to-survey volume ratio and then subtracted to the GSMF of the member-candidate galaxies to obtain the GSMF of the (bona fide) member galaxies of each fossil group. Counts per stellar mass bin are normalized to the total mass M_{200} of each fossil group, to enable comparison with the composite GSMF of the 40 (11) *COSMOS* X-ray selected groups at $0.3 \leq z \leq 0.5$ with $2 \times 10^{13} \leq M_{200} \leq 5 \times 10^{13} M_{\odot}$ ($M_{200} > 5 \times 10^{13} M_{\odot}$) from Giodini et al. (in preparation). These two composite GSMFs are computed in an analogous way, but include the number counts from all selected groups with similar masses to that of either fossil group; they are normalized to the sum of the total masses of the individual groups.

Figure 3 shows the normalized GSMFs of the two fossil groups and the normalized composite GSMFs of the two reference samples of X-ray selected groups at $0.3 \leq z \leq 0.5$ for all (bona fide) member galaxies and for those classified as passively evolving. Comparison of these normalized GSMFs reveals that about 80% of the galaxies with $M^{\text{stars}} \geq 10^{10} M_{\odot}$ are passively evolving in the two fossil groups at $z \approx 0.4$. Conversely, passive galaxies start dominate the GSMF of the coeval, mass-complete sample of

X-ray selected groups at much higher stellar masses, with a fraction of 80% passive galaxies being reached only at $M^{\text{stars}} \geq 10^{11} M_{\odot}$. This holds although the fraction of passively evolving galaxies increases towards larger stellar masses across the entire range in stellar mass.

Interestingly, half of the galaxies with $M^{\text{stars}} \sim 10^{11} M_{\odot}$ do not show evidence of ongoing star-formation activity for similarly massive, optically selected groups at $0.3 \leq z \leq 0.48$ (Wilman et al. 2008)¹².

If the fraction of star-forming (“blue”) galaxies is a proxy for the dynamical youth of a galaxy system at fixed total mass (e.g., Tully & Shaya 1984; Balogh, Navarro, & Morris 2000; Ellingson et al. 2001; Zapata et al. 2009; Braglia et al. 2009), the previous difference suggests that the two fossil groups assembled their DM haloes earlier than the average system among the similarly massive groups at $0.3 \leq z \leq 0.5$.

3.2 Colour–magnitude diagram

The dominance of passively evolving or quiescent galaxies at $M^{\text{stars}} \geq 10^{10} M_{\odot}$ is confirmed, in a more direct way, by the $b-r$ vs i colour–magnitude diagram of either fossil group (see Fig. 4). This diagram is obtained using Subaru photometry (see Ilbert et al. 2009). For $z \sim 0.4$, the $b-r$ colour nicely brackets the redshifted spectral feature at $\sim 4000 \text{ \AA}$ (rest frame), whose amplitude increases together with the time since the last main episode of star formation but also with increasing metallicity (e.g. Worthey 1994).

Both fossil groups exhibit a well defined red-sequence, and a lack of galaxies within $0.5 R_{200}$ that are bluer than this locus by ≥ 0.5 mag. Most of these blue galaxies are at least ~ 4 magnitudes fainter than the BCG of either fossil group in the i -band. Moving out to R_{200} , the bona fide member galaxies with a $b-r$ colour at least 0.5 mag bluer than the BCG one are still a few. This confirms that most of the luminous galaxies within the bound region of either fossil group are old and passively evolving or quiescent, modulo dust attenuation (cf. Wilman et al. 2008).

The dominance of galaxies with a very low star-formation activity among those that are about two to four magnitudes fainter than the BCG is confirmed for the fossil groups RXC J2315.7–0222 and RXC J0216.7–4749

¹¹ *COSMOS* galaxies are classified as passively evolving or star forming on the basis of the template best-fitting their individual SEDs. In particular, the former galaxies have star formation rates lower than $10^{-2} M_{\odot} \text{ yr}^{-1}$.

¹² In Wilman et al. (2008), passive galaxies are defined on the basis of their *Spitzer*-IRAC mid-infrared colours, stellar masses are derived from rest-frame K-band luminosities (in analogy with Ilbert et al. 2009).

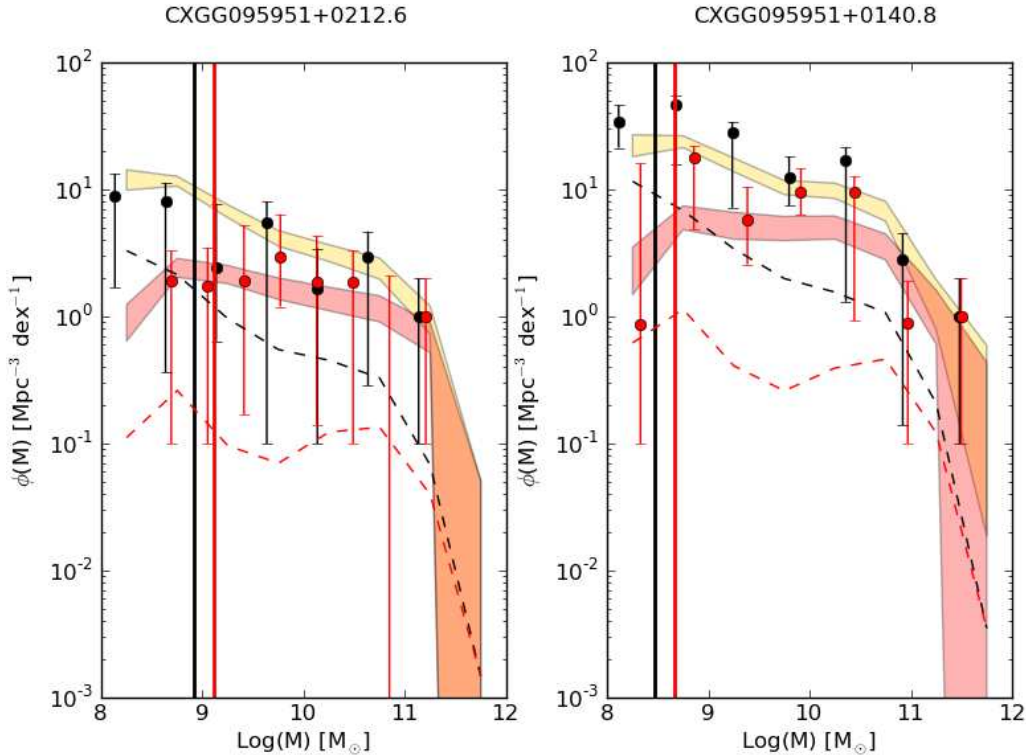


Figure 3. The galaxy stellar mass functions (GSMFs) of the two fossil groups CXGG 095951+0212.6 (left) and CXGG 095951+0140.8 (right). Each panel shows the GSMF for all the (bona fide) member galaxies (black circles) and the GSMF for the subsample of passively evolving (bona fide) member galaxies (red symbols), together with their statistical uncertainties. Conversely, the vertical black and red lines represent, respectively, the mass completeness limit for all the galaxies at the same redshift as the group and for the passively evolving ones among them. In each panel the black and red dashed curves represent, respectively, the GSMFs for all the galaxies in the coeval field and for the passively evolving ones among them. To obtain the GSMF of all the (bona fide) member galaxies of either group, the corresponding field GSMF was normalized by the group-to-survey volume ratio and then subtracted to the GSMF of all the candidate members. The GSMF of the passively evolving (bona fide) member galaxies of either group was obtained in an analogous way. Furthermore, each panel shows the composite GSMFs of the coeval, X-ray selected groups for all their (bona fide) member galaxies (yellow area) and the passively evolving ones among them (red area) together with their statistical uncertainties (Giodini et al. in preparation). Among the X-ray selected groups at $0.3 \leq z \leq 0.5$ in *COSMOS*, there are 40 systems as massive as CXGG 095951+0212.6 (i.e., with $2 \times 10^{13} \leq M_{200} \leq 5 \times 10^{13} M_{\odot}$) and 11 systems as massive as CXGG 095951+0140.8 (i.e., with $M_{200} > 5 \times 10^{13} M_{\odot}$).

(Démoclès et al. 2010), AWM4 (Zibetti et al. 2009; see fig. 2 in Koranyi & Geller 2002), RX J1416.4+2315 (see fig. 2 in Cypriano, Mendes de Oliveira, & Sodr  2006), and the fossil group candidate RX J1520.9+4840¹³ (Eigenthaler & Zeilinger 2009). However, in the literature there is no comparative study of the galaxy populations of fossil and non-fossil systems of similar masses down to such fainter magnitudes, based on multi-band photometry or spectroscopy.

Finally, we note that two member-candidate galaxies with $i \approx 23.4$ and $i \approx 24.1$ exhibit colors that are much redder than average color of the red-sequence of CXGG 095951+0140.8 ($b - r \approx 2.3$ and $b - r \approx 2.9$, respectively, vs $b - r \approx 1.7$). These two very faint and red galaxies (about 6.3–7 i -mag fainter and 0.4–1 mag redder in $b - r$ than the BCG) are located at projected distances of 110 and 330 kpc from the BCG (or the cluster center), respectively. Member-candidate galaxies with analo-

gous photometric properties exist in the fossil group candidate RX J1548.9+0851¹⁴ (Eigenthaler & Zeilinger 2009).

4 DISCUSSION

4.1 Characteristic timescales

In order to understand why the bulk of the galaxies with $M^{\text{stars}} \geq 10^{10} M_{\odot}$ are dominated by old, passively evolving stellar populations in the two fossil groups at $z \approx 0.4$, we need to estimate if there was enough time for the last formed stars to age once their host galaxy had reached the bound region of either group. Hence, we need to estimate the following timescales: the time elapsed since half the DM halo of each fossil group was in place (i.e., the so-called “assembly time”), and the time elapsed since the last significant infall of blue galaxies with $M^{\text{stars}} \geq 10^{10} M_{\odot}$ occurred. These two

¹³ For this object the virial radius was estimated on the basis of a scaling relation (Evrard, Metzler & Navarro 1996).

¹⁴ The fossil nature of this group comes under scrutiny however (P. Eigenthaler private communication).

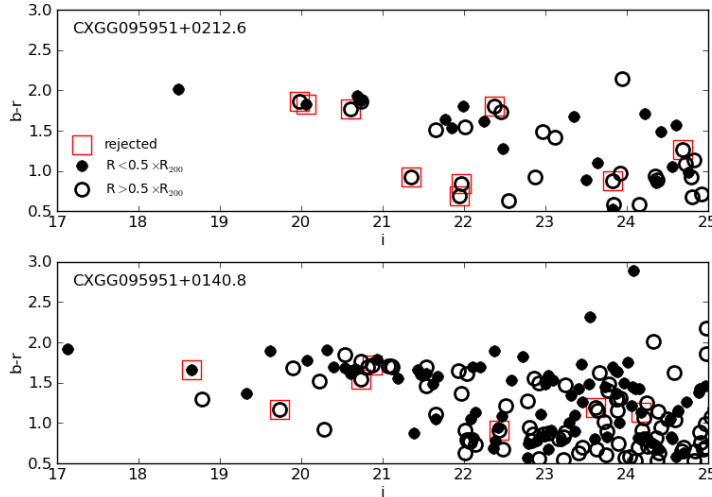


Figure 4. $b-r$ vs i colour-magnitude diagram (observed frame) for all member-candidate galaxies of either fossil group (black circles); galaxies within a group-centric distance of $0.5R_{200}$ are marked by filled circles. Red open squares mark those photometric-member galaxies with a spectroscopic redshift inconsistent with that of either group (see Sect. 2).

timescales need to be compared with the minimum life-time of the stellar populations characterizing old, passively evolving (i.e., red-sequence) galaxies, which is about 1–2 Gyr.

We now make the conservative assumption that the two fossil groups behave as other similarly massive groups observed at $z \approx 0.4$. Furthermore, we assume that groups do not significantly increase their total masses between $z \approx 0.5$ and $z \approx 0.4$ ¹⁵, in a statistical sense. By doing so, we can use results on the median formation redshifts of DM haloes obtained from the simulations of Gao et al. (2004) or different analytical models that are reproduced in fig. 5 of Giocoli et al. (2007). Groups of similar total masses to CXGG 095951+0212.6 and CXGG 095951+0140.8 have assembled half of their DM halo at typical redshifts of ~ 1.2 and ~ 1.05 , respectively, which correspond to similar look-back times of ≈ 4 Gyr at $z = 0.425$ and $z = 0.372$.

According to the computations of dynamical friction and galaxy-merging timescales of Boylan-Kolchin, Ma & Quataert (2008, their fig. 1), galaxies with $M^{\text{stars}} \sim 10^{10}$ or $10^{11} M_{\odot}$ need about 6 or 3 Gyr, respectively, to reach an orbit with maximum group-centric distance of $0.5R_{200}$ from R_{200} for the first time. Since the simulations of Boylan-Kolchin et al. mostly neglect the effect of the central galaxy in a given DM halo on the merging time-scale, and do not take into account the drag on ambient gas (e.g. Ostriker 1999), we infer that the epoch of last infall of blue galaxies with $M^{\text{stars}} \geq 10^{10} M_{\odot}$ can date back to less than 3–6 Gyr with respect to the lookback time of either fossil group.

The time of last infall of blue, intermediate-mass galaxies is comparable to the median time elapsed since the assembly of a group as massive as either fossil group, if not longer than that. Thus, we can assume that most of the galaxies with $M^{\text{stars}} \geq 10^{10} M_{\odot}$ have resided within the

bound region of either fossil group since its assembly (cf. von Benda-Beckmann et al. 2008; Dariush et al. 2010). This “residence” time of ≈ 4 Gyr is longer than the typical life-times of young stars, which are responsible for the bulk luminosity shortward of the 4000 Å-break, when they are present. Hence, there is enough time to observe a dominating population of old, passively evolving galaxies with $M^{\text{stars}} \geq 10^{10} M_{\odot}$ in the two fossil groups at $z \approx 0.4$. This is even more the case if the assembly time of a fossil group is shorter than the median assembly time for all coeval, similarly massive groups (D’Onghia et al. 2005; Dariush et al. 2007). Environmental effects could be responsible for the raise of the population of old, passively evolving galaxies in the two fossil groups (see Boselli & Gavazzi 2006 for a recent review).

4.2 Star formation history

Member-candidate galaxies of either fossil group which are satellites at $z \approx 0.4$ could reach stellar masses of $1-8 \times 10^{10} M_{\odot}$ before their star formation turned to its end. We note that, in spite of the generally held, negative feedback exerted by the group environment on the star formation activity of member galaxies, such an activity seems to be enabled in 20%–50% of the galaxies with $M^{\text{stars}} \sim 10^{11} M_{\odot}$ in groups at similar redshifts and with similar masses (Fig. 2; Giodini et al. in preparation; see also Wilman et al. 2008 and references therein).

It is easy to understand how tidal interactions¹⁶ (e.g., Spitzer & Baade 1951; Richstone 1976; Farouki & Shapiro

¹⁵ According to the adopted cosmological model (Sect. 1), this redshift range corresponds to a time interval of 0.7 Gyr.

¹⁶ Tidal interaction may have been active in a de-localized way, in particular during the process of rapid and violent formation of the dominant galaxy (D’Onghia et al. 2005; see also Pierini et al. 2008 for an analogy), but, also, in a more localized way, since the early formation of the central dominant galaxy (see Elmegreen et al. 2000 for an analogy).

1981; Merritt 1983, 1984; Icke 1985; Miller 1986; Byrd & Valtonen 1990; Valluri & Jog 1990) or harassment (Moore et al. 1996) could have inhibited the growth of satellite galaxies up to $M^{\text{stars}} \sim 10^{10} M_{\odot}$. It is less certain how the same interaction processes¹⁷ could have fostered the growth of more massive satellite galaxies (e.g., Keel et al. 1985; Kennicutt et al. 1987; Byrd & Valtonen 1990; Mihos et al. 1992; Henriksen & Byrd 1996; Lake, Katz & Moore 1998; Iono, Yun & Mihos 2004; Braglia, Pierini & Böhringer 2007).

An earlier assembly time of fossil groups with respect to non-fossil groups of similar masses (D’Onghia et al. 2005; Dariush et al. 2007) can justify the lower fraction of star-forming galaxies with $10^{10} \leq M^{\text{stars}} \leq 10^{11} M_{\odot}$ (see Sect. 4.1). As discussed by D’Onghia et al. (2005), this is also consistent with the larger X-ray-to-optical luminosity ratios of fossil groups with respect to similarly massive non-fossil groups in the local Universe claimed by Jones et al. (2003). In fact, in groups with earlier assembly times the hot gas was collected and started cooling earlier and at higher central densities. However, no difference in the scaling relation between X-ray and optical luminosities is reported for a sample of seven fossil groups at $z \leq 0.2$ and total masses M_{200} of a few times $10^{14} M_{\odot}$ (Voevodkin et al. 2010), at variance with previous results (Jones et al. 2003; Khosroshahi et al. 2007). As mentioned in Sect. 2, the X-ray-to-optical luminosity ratio is rather high for CXGG 095951+0140.8 but normal for CXGG 095951+0212.6, when compared to those of similarly massive groups at $z = 0.3$ – 0.5 .

Interestingly, there is growing evidence that an environment characterized by high galaxy number density and low galaxy velocity dispersion, such as the one found in compact groups, plays a key role in accelerating galaxy evolution by enhancing star-formation processes in galaxies and favoring a fast transition to quiescence (Tzanavaris et al. 2010; Walker et al. 2010 and references therein). Such an environment could represent the immediate progenitor of a fossil system. This is straightforward if such a progenitor is a compact group, and compact groups are interpreted as transient phases in the dynamical evolution of looser groups (Barnes 1989). Alternatively, an environment with the previous characteristics can be produced if the existence of fossil systems is primarily driven by the relatively early infall of massive satellites (D’Onghia et al. 2005; von Benda-Beckmann et al. 2008). Tentatively this may be achieved through preferential infall on orbits with typically lower angular momentum. Consistently, there is an indication of the presence of galaxies in radial orbits in the external region of the fossil cluster RX J105453.3+552102 (Aguerri et al. 2011).

In a future study, we will explore if an efficient confinement of the hot, X-ray emitting gas (Mathews et al. 2005) could foster the rather large stellar mass fractions of the two fossil groups under study (cf. G09).

4.3 Fossil group progenitors

An earlier assembly time for fossil groups with respect to as massive non-fossil groups is consistent with the obser-

vational results discussed in Sect. 3; it is also predicted by simulations in a statistical sense (D’Onghia et al. 2005; Dariush et al. 2007). The evidence is a GSMF dominated by old, passively evolving systems at $M^{\text{stars}} \geq 10^{10} M_{\odot}$ (Sect. 3.1) plus the corresponding existence of a tight red-sequence (Sect. 3.2). Since the two fossil groups at $z \approx 0.4$ sit in very different density environments of the LSS (Sect. 2), the conditions leading to the formation of a fossil system, in particular to the shaping of its galaxy population, do not appear to be intimately connected to the surrounding LSS. This is also consistent with simulations (von Benda-Beckmann et al. 2008; Cui et al. 2011).

An early formation time was advocated by Aguerri et al. (2011) to explain the dynamics and luminosity function of the member galaxies as well as the photometric properties of the BCG for the relaxed, massive ($M_{200} \sim 1 \times 10^{15} M_{\odot}$) fossil system RX J105453.3+552102 at $z = 0.47$. On the other hand, a deep optical image of the BCG of the low X-ray luminosity fossil-group candidate RX J1548.9+0851 (Santos, Mendes de Oliveira & Sodré 2007) clearly reveals the existence of many shells (Eigenthaler & Zeilinger 2009). According to Hernquist & Spergel (1992), many shell systems among elliptical and spheroidal galaxies may have originated through major mergers of disc galaxies with comparable masses rather than via minor mergers - between a massive elliptical galaxy and a small disc companion (Quinn 1984; Hernquist & Quinn 1988, 1989) or a small elliptical/spiral companion (Dupraz & Combes 1986) - or accretions (Thomson & Wright 1990; Thomson 1991). We speculate that the relatively early infall of massive satellites can better justify the formation of a rather massive fossil group in a denser region of the LSS, like CXGG 095951+0140.8, whereas compact groups can more likely be the progenitors of observed low-mass and isolated fossil groups, like CXGG 095951+0212.6.

On one hand, the LSS surrounding the progenitor of a fossil group could be responsible more for the growth of the total mass of the system than for the growth of the stellar mass of its BCG (see Khosroshahi, Ponman & Jones 2006). This is consistent with both the shallow dependence of the median luminosity of BCGs on the total mass of the parent halo observed in the local Universe (Yang, Mo & van den Bosch 2008) and the result from the hydrodynamic simulations of Cui et al. (2011) that X-ray bright groups are disproportionately rare in low-density regions.

On the other hand, it is reasonable to assume that isolated fossil groups can be identified as such for longer times than non isolated ones of similar mass, because it is more difficult either that their magnitude gap is replenished by infalling galaxies, or that they fall into larger bound structures. In a low density environment, a loose group has more chances to keep its identity and dynamically evolve into a fossil group after a compact group phase (cf. Barnes 1989). Either in the case of early assembly (D’Onghia et al. 2005; Dariush et al. 2007) or in the case of final evolution of a loose group (Barnes 1989), a rapid build-up of the stellar mass and the following quick end of the star-formation activity in most of the brightest member galaxies need to be invoked. Interestingly, this is what compact groups in the local Universe seem to have experienced (Tzanavaris et al. 2010; Walker et al. 2010 and references therein).

If two channels lead to the formation of a fossil group

¹⁷ Tidal interactions and harassment describe, respectively, prolonged and collective impulsive interactions of type galaxy–galaxy or galaxy–gravitational potential well of the parent system.

and there is a sort of density environment bias on identification and inference on the progenitor from observations, the stellar populations of the BCG of a fossil group do not necessarily have to be remarkably different from those of field, massive early-type galaxies of similar optical and X-ray luminosities at $z \sim 0$ (cf. La Barbera et al. 2009). Furthermore, the size of environmental effects on typical red-sequence galaxies is still a controversial issue, and might be quite small at large stellar masses (cf. e.g., Thomas et al. 2005, 2010; Pannella et al. 2009; Cooper et al. 2010). Hence, there might be less tension between our conclusions and the result of La Barbera et al. (2009)¹⁸.

Future multi-wavelength studies of statistical samples of fossil groups with different masses and redshifts (e.g., Santos et al. 2007), located in different density regions of the LSS, will provide a test of our interpretation and hypotheses.

4.4 Intracluster light

Here we discuss if the contribution from low-surface brightness, diffuse stellar emission not associated with galaxies (the so-called intracluster light - ICL) could explain the rather low value of L_i/L_X found in Sect. 2 for the more massive fossil group, CXGG 095951+0140.8. The impact on the total stellar mass budget of the ICL has already been pointed out in the literature, and with different scales, from observations (cf. e.g., Zibetti et al. 2005 and Gonzalez et al. 2007). In simulations, most of the ICL seems to be associated with the build-up of the BCG (e.g., Murante et al. 2007 and references therein). The expected amount of ICL is uncertain as well as the observed one - 3% to 30% of all stars in groups at $z = 0$ (e.g., Kapferer et al. 2010 and references therein) - and seems to be independent of the mass-scale of the galaxy system (e.g., Dolag, Murante & Borgani 2010 and references therein).

Groups of galaxies that formed early (as fossil groups, potentially) might be particularly effective at producing ICL, as interactions in the group environment begin to liberate tidal material. Galaxy systems as massive as the two fossil groups under study have smaller velocity dispersions than do massive clusters, meaning that interactions on the group scales can be slow and damaging as opposite to the impulsive high speed encounters, e.g. by harassment, on the cluster scale. These slow tidal interactions can strip material from rotating disc galaxies into loosely bound tidal structures, forming long tails of stars and gas (D’Onghia et al. 2009). It is then interesting to estimate this additional amount of unbound stars that can escape detection in the present data.

In particular, we use the approximations developed in D’Onghia et al. (2010) to compute the fraction of ICL that a disc galaxy with a dynamical mass equal to $5 \times 10^{11} M_\odot$ (of which $2 \times 10^{10} M_\odot$ is in the disc) produces passing on a parabolic orbit within the potential of a typical group. Such a galaxy has a stellar mass of the order of $10^{10} M_\odot$. Figure 5 shows that the smaller the pericentric distance the larger the fraction of light stripped into the intergalactic medium. The

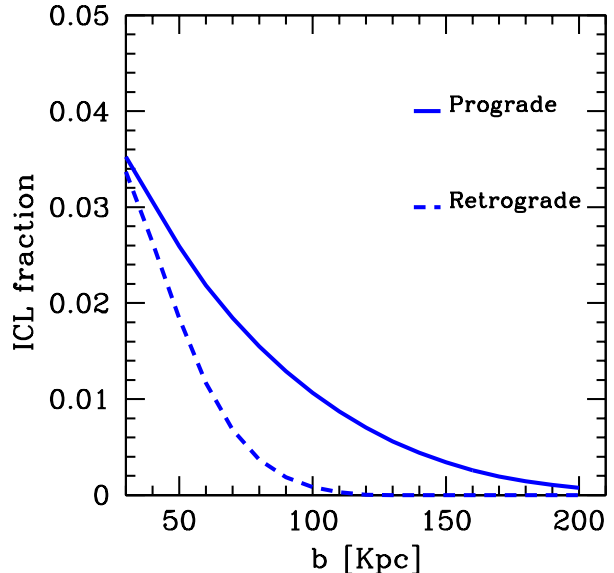


Figure 5. The fraction of ICL released by the model galaxy (see text) orbiting within the potential of a typical group computed as a function of pericentric distance (from D’Onghia et al. 2010). Due to the quasi-resonance phenomenon of the tidal interaction, the prograde encounters are more efficient in stripping material than the retrograde ones.

fraction of ICL computed for the model galaxy is given by the ratio of the number of unbound stars to the total amount of stars bound to all the galaxies of the group. This galaxy, passing at 30-40 kpc from the group center, can contribute up to 3% of the total light in the group galaxies. Hence, slow tidal interactions likely provide a marginal contribution to the total stellar budget of a low-mass fossil group as CXGG 095951+0212.6, but a non-negligible one for a fossil group as massive as CXGG 095951+0140.8. Given these rough estimates, we will estimate the ICL contribution to the total stellar luminosity of the two fossil groups under study in the future, thanks to the deep B- and R-band photometry recently obtained by us with the Wide Field Imager (Baade et al. 1999), mounted at the Cassegrain focus of the MPG/ESO 2.2 m telescope in La Silla, Chile.

5 CONCLUSIONS

For the first time, the galaxy stellar mass function (GSMF) was computed, down to a stellar mass $M^{\text{stars}} \sim 10^9 M_\odot$ and in a robust statistical way, for two fossil groups discovered at $z \approx 0.4$: CXGG 095951+0212.6 and CXGG 095951+0140.8. These groups have also well-determined total masses (M_{200}) equal to $1.9 (\pm 0.41) \times 10^{13}$ and $9.5 (\pm 0.42) \times 10^{13} M_\odot$, respectively. This was possible because of the high-quality multi-wavelength information available for the 2 deg^2 area of the Cosmic Evolution Survey (COSMOS; Scoville et al. 2007) where the two systems were initially detected in X-rays (Finoguenov et al. in preparation; G09). In particular, the identification as fossil and the selection of the member-candidate galaxies of either group rest on robust photometric redshifts, and $i_{AB} \leq 22.5$ mag limited spectroscopy.

¹⁸ In addition, we note that comparison of models and observations is not straightforward even when considering simple stellar population models (Conroy & Gunn 2010 and references therein).

Interestingly, the large-scale structure (LSS) in which the two fossil groups are embedded is very different: CXGG 095951+0212.6 appears isolated, whereas CXGG 095951+0140.8 belongs to a LSS that covers the entire 2 deg^2 area of the COSMOS (corresponding to a cross size of about 25.5 Mpc at $z \approx 0.4$) and is traced by a total of 28 X-ray emitting groups.

Comparison of the GSMF of these fossil groups and the composite GSMF of the COSMOS X-ray emitting groups at $0.3 \leq z \leq 0.5$ that span a similar range in total mass (Giodini et al. in preparation) highlights a lack of star-forming galaxies with $M^{\text{stars}} \geq 10^{10} M_{\odot}$ in the two fossil groups. Consistently, the distribution of their photometric member galaxies in the $b-r$ vs i colour-magnitude diagram reveals a well-defined red sequence and a lack of significantly bluer, luminous galaxies out to the virial radius R_{200} of either fossil group. In addition, the total stellar mass fraction of these groups within $0.7R_{200}$ is relatively large for their total masses (G09), in particular for the less massive one (i.e., CXGG 095951+0212.6).

This evidence suggests that the overall conversion of (cold) gas into stars was accelerated and/or more efficient in fossil groups with respect to the average X-ray emitting group in the same mass range and at similar redshift. The star-formation activity in member galaxies rapidly ceased afterwards. At the same time, no significant infall of galaxies with $M^{\text{stars}} \geq 10^{10} M_{\odot}$ took place in the last 3–6 Gyr for either fossil group at $z \approx 0.4$.

If the processes shaping the galaxy component of a fossil group seem to be independent of the LSS, the progenitor of an observed fossil group may depend on it. On the basis of the measured stellar mass fractions (G09) and X-ray-to-optical luminosity ratios (Giodini et al. in preparation), we propose that compact groups are the most likely progenitors of observed low mass and isolated fossil groups, like CXGG 095951+0212.6. Conversely, the relatively early infall of massive satellites likely originates massive fossil groups in dense regions of the LSS, like CXGG 095951+0140.8.

ACKNOWLEDGMENTS

We thank the referee, Paul Eigenthaler, for a careful reading of the original version of the paper and the useful comments that improved the presentation of the paper. DP acknowledges the kind and fruitful hospitality at the Max-Planck-Institut für extraterrestrische Physik (MPE).

REFERENCES

- Aguerre J.A.L. et al. 2011, A&A, 527, 143
 Arimoto N., Yoshii, Y. 1987, A&A, 173, 23
 Baade D. et al. 1999, MNRAS, 308, 15
 Balogh M.L., Navarro J.F., Morris S.L., 2000, ApJ, 540, 113
 Barnes J.E., 1989, Nature, 338, 123
 Boselli A., Gavazzi G., 2006, PASP, 118, 517
 Boyle-Kolchin M., Ma C.-P., Quataert E., 2008, MNRAS, 383, 93
 Braglia F.G., Pierini D., Böhringer H., 2007, A&A, 470, 425
 Braglia F.G., Pierini D., Biviano A., Böhringer H., 2009, A&A, 500, 947
 Byrd G., Valtonen M., 1990, ApJ, 350, 89
 Chabrier G., 2003, ApJ, 586, L133
 Conroy C., Gunn J.E., 2010, ApJ, 712, 833
 Cooper M.C., Gallazzi A., Newman J.A., Yan R., 2010, MNRAS, 402, 1942
 Cui W., Springel V., Yang X., De Lucia G., Borgani S., 2011, MNRAS, in press (arXiv:1102.4269)
 Cypriano E.S., Mendes de Oliveira C.L., Sodr  L. Jr., 2006, AJ, 132, 514
 Dariush A., Khosroshahi H.G., Ponman T.J., Pearce F., Raychaudhury S., Hartley W., 2007, MNRAS, 382, 433
 Dariush A., Raychaudhury S., Ponman T.J., Khosroshahi H.G., Benson A.J., Bower R.G., Pearce F., 2010, MNRAS, 405, 1873
 D mocl s J., Pratt G.W., Pierini D., Arnaud M., Zibetti S., D’Onghia E., 2010, A&A, 517, 52
 Dolag K., Murante G., & Borgani S., 2010, MNRAS, 405, 1544
 D’Onghia E., Lake G., 2004, ApJ, 612, 628
 D’Onghia E., Sommer-Larsen J., Romeo A.D., Burkert A., Pedersen K., Portinari L., Rasmussen J., 2005, ApJ, 630, L109
 D’Onghia E., Besla G., Cox T.J., Hernquist L., 2009, Nature, 460, 605
 D’Onghia E., Vogelsberger M., Figuere-Ciguere C., Hernquist L., 2010, ApJ, 725, 353
 Dunkley J. et al., 2009, ApJS, 180, 306
 Dupraz C., Combes F., 1986, A&A, 166, 53
 Eigenthaler P., Zeilinger W. W., 2009, Astronomische Nachrichten, 330, 978
 Ellingson E., Lin H., Yee H.K.C., Carlberg R.G., 2001, ApJ, 547, 609
 Elmegreen D.M., Elmegreen B.G., Chromey F.R., Fine M.S., 2000, AJ, 120, 733
 Evrard A.E., Metzler C.A., Navarro J.F., 1996, ApJ, 469, 494
 Farouki R., Shapiro S.L., 1981, ApJ, 243, 32
 Finoguenov A. et al. 2007, ApJS, 172, 182
 Gao L., White S.D.M., Jenkins A., Stoehr F., Springel V., 2004, MNRAS, 355, 819
 Giocoli C., Moreno J., Sheth R.K., Tormen, G., 2007, MNRAS, 376, 977
 Giodini S. et al. 2009, ApJ, 703, 982 (G09)
 Giodini S. et al. 2010, ApJ, 714, 218
 Gonzalez A.H., Zabludoff A.I., Zaritsky D., 2007, ApJ, 666, 147
 Henriksen M., Byrd, G., 1996, ApJ, 459, 82
 Hernquist L., Quinn P.J., 1988, ApJ, 331, 682
 Hernquist L., Quinn P.J., 1989, ApJ, 342, 1
 Hernquist L., Spergel D.N., 1992, ApJ, 399, L117
 Icke V., 1985, A&A, 144, 115
 Ilbert O. et al., 2009, ApJ, 690, 1236
 Iono D., Yun M.S., Mihos J.C., 2004, ApJ, 616, 199
 Jones L.R., Ponman T.J., Forbes D.A., 2000, MNRAS, 312, 139
 Jones L.R., Ponman T.J., Horton A., Babul A., Ebeling H., Burke D.J., 2003, MNRAS, 343, 627
 Kapferer W., Schindler S., Knollmann S.R., van Kampen E., 2010, A&A, 516, 41
 Keel W.C., Kennicutt R.C. Jr., Hummel E., van der Hulst

- J.M., 1985, *AJ*, 90, 708
- Kennicutt R.C. Jr., Roettiger K.A., Keel W.C., van der Hulst J.M., Hummel E., 1987, *AJ*, 93, 1011
- Khosroshahi H.G., Ponman, T.J., Jones L.R., 2006, *MNRAS*, 372, 68
- Khosroshahi H.G., Ponman, T.J., Jones L.R., 2007, *MNRAS*, 377, 595
- Knobel C. et al., 2009, *ApJ*, 697, 1842
- Koekemoer A.M. et al., 2007, *ApJS*, 172, 196
- Komatsu E. et al., 2009, *ApJS*, 180, 330
- Koranyi D.M., Geller M.J., 2002, *AJ*, 123, 100
- La Barbera F., de Carvalho R.R., de la Rosa I.G., Sorrentino G., Gal R.R., Kohl-Moreira J.L., 2009, *AJ*, 137, 3942
- Lake G., Katz N., Moore B., 1998, *ApJ*, 495, 152
- Leauthaud A. et al., 2010, *ApJ*, 709, 97
- Lilly S.J. et al., 2007, *ApJS*, 172, 70
- Mathews W.G., Faltenbacher A., Brighenti F., Buote D.A., 2005, *ApJ*, 634, L137
- Merritt D., 1983, *ApJ*, 264, 24
- Merritt D., 1984, *ApJ*, 276, 26
- Mihos J.C., Richstone D.O., Bothun G.D., 1992, *ApJ*, 400, 153
- Miller R.H., 1986, *A&A*, 167, 41
- Milosavljević M., Miller C.J., Furlanetto S.R., Cooray A., 2006, *ApJ*, 637, L9
- Moore B., Katz N., Lake G., Dressler A., Oemler A., 1996, *Nature*, 379, 613
- Murante G., Giovalli M., Gerhard O., Arnaboldi M., Borgani S., Dolag K., 2007, *MNRAS*, 377, 2
- Ostriker E.C., 1999, *ApJ*, 513, 252
- Pannella M. et al., 2009, *ApJ*, 701, 787
- Pierini D., Maraston C., Bender R., Witt A.N., 2004, *MNRAS*, 347, 1
- Pierini D., Zibetti S., Braglia F., Böhringer H., Finoguenov A., Lynam P.D., Zhang Y.-Y., 2008, *A&A*, 483, 727
- Ponman T.J., Bertram D., 1993, *Nature*, 363, 51
- Ponman T.J., Allan D.J., Jones L.R., Merrifield M., McHardy I.M., Lehto H.J., Luppino G.A., 1994, *Nature*, 369, 462
- Quinn P.J., 1984, *ApJ*, 279, 596
- Richstone D.O., 1976, *ApJ*, 204, 642
- Romer A.K. et al. 2000, *ApJS*, 126, 209
- Sales L.V., Navarro J.F. Lambas D.G., White S.D.M., Croton D.J., 2007, *MNRAS*, 382, 1901
- Salpeter E.E., 1955, *ApJ*, 121, 161
- Santos W.A., Mendes de Oliveira C., Sodré L. Jr., 2007, *AJ*, 134, 1551
- Schechter P., 1976, *ApJ*, 203, 297
- Schirmer M., Suyu S., Schrabback T., Hildebrandt H., Erben T., Halkola A., 2010, *A&A*, 514, 60
- Scoville N. et al., 2007, *ApJS*, 172, 1
- Spitzer L. Jr., Baade W., 1951, *ApJ*, 113, 413
- Sun M., Voit G.M., Donahue M., Jones C., Forman W., Vikhlinin A., 2009, *ApJ*, 693, 1142
- Teyssier R., Moore B., Martizzi D., Dubois Y., Mayer L., 2011, *MNRAS*, 414, 195
- Thomas D., Maraston C., Bender R., Mendes de Oliveira C., 2005, *ApJ*, 621, 673
- Thomas D., Maraston C., Schawinsk, K., Sarzi M., Silk J., 2010, *MNRAS*, 404, 1775
- Thomson R.C., 1991, *MNRAS*, 253, 256
- Thomson R.C., Wright A.E., 1991, *MNRAS*, 247, 122
- Tully R.B., Shaya E.J., 1984, *ApJ*, 281, 31
- Tzanavaris P. et al., 2010, *ApJ*, 716, 556
- Valluri M., Jog C.J., 1990, *ApJ*, 357, 367
- Vikhlinin A., McNamara B.R., Hornstrup A., Quintana H., Forman W., Jones C., Way M., 1999, *ApJ*, 520, L1
- Voevodkin A., Borozdin K., Heitmann K., Habib S., Vikhlinin A., Mescheryakov A., Hornstrup A., Burenin R., 2010, *ApJ*, 708, 1376
- von Benda-Beckmann A.M., D’Onghia E., Gottlöber S., Hoeft M., Khalatyan A., Klypin A., Müller V., 2008, *MNRAS*, 386, 2345
- Walker L.M., Johnson K.E., Gallagher S.C., Hibbard J.E., Hornschemeier A.E., Tzanavaris P., Charlton J.C., Jarrett T.H., 2010, *AJ*, 140, 1254
- Wilman D.J. et al., 2008, *ApJ*, 680, 1009
- Worthey G., 1994, *ApJS*, 95, 107
- Yang X., Mo H.J., van den Bosch F.C., 2008, *ApJ*, 676, 248
- Zapata T., Perez J., Padilla N., Tissera P., 2009, *MNRAS*, 394, 2229
- Zibetti S., White S.D.M., Schneider D.P., Brinkmann J., 2005, *MNRAS*, 358, 949
- Zibetti S., Pierini D., Pratt G.W. 2009, *MNRAS*, 392, 525

This paper has been typeset from a \LaTeX file prepared by the author.